Visualization and Interaction Techniques for the Exploration of Vascular Structures

Horst K. Hahn, Bernhard Preim, Dirk Selle und Heinz-Otto Peitgen

MeVis – Center for Medical Diagnostic Systems and Visualization, Bremen, Germany

Abstract

We describe a pipeline of image processing steps for deriving symbolic models of vascular structures from radiological data which reflect the branching pattern and diameter of vessels. For the visualization of these symbolic models, concatenated truncated cones are smoothly blended at branching points. We put emphasis on the quality of the visualizations which is achieved by anti-aliasing operations in different stages of the visualization. The methods presented are referred to as HQVV (High Quality Vessel Visualization). Scalable techniques are provided to explore vascular structures of different orders of magnitude. The hierarchy as well as the diameter of the branches of vascular systems are used to restrict visualizations to relevant subtrees and to emphasize parts of vascular systems.

Our research is inspired by clear visualizations in textbooks and is targeted toward medical education and therapy planning. We describe the application of vessel visualization techniques for liver surgery planning. For this application it is crucial to recognize the morphology and branching pattern of vascular systems as well as the basic spatial relations between vessels and other anatomic structures.

CR Categories and Subject Descriptors: I.3.3 [Computer Graphics]: Methodology and Techniques – Antialiasing, I.3.6 [Computer Graphics]: Methodology and Techniques – Interaction Techniques, J.3 [Computer Applications]: Life and Medical Sciences

Additional Keywords: vessel visualization, medical visualization, computer-assisted surgery

1 INTRODUCTION

Understanding the branching pattern of tree-like vascular structures inside the human body is a crucial aspect of medical education and many therapy planning tasks. For diagnosis or therapy planning, it is of paramount importance to recognize shape features and morphology of vascular structures as well as spatial relations between vessels and other relevant structures. Due to the limited resolution of CT- and MR-scanners which provide the image data for therapy planning, conventional visualizations show artifacts from partial volume effects and high-frequency noise, particularly for small vessels whose diameters grow and shrink from slice to slice [GER93].

Depending on the quality of the acquired data, vascular systems might be rather small (in some cases only 20 branchings can be extracted) or complex (with several thousand branchings). Moreover, some organs possess several vascular systems. For example, the liver has portal veins, liver arteries, hepatic veins and biliary ducts.

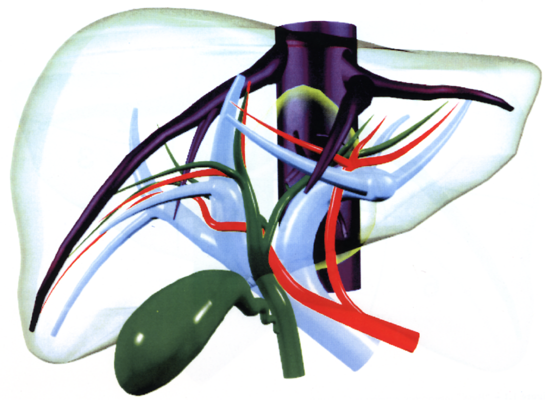

Figure 1: Vascular structures of the human liver. (From [MAZ97]).

Figure 1 presents a hand-drawn illustration of these vascular structures from a well-known textbook on surgery which inspired our work [MAZ97]. Notice that smooth visualizations of the vessels make it easy to interpret the branching pattern and geometric properties such as vessel diameter and curvature.
The following objectives guided our work:

- *To reconstruct a symbolic vascular model*. Annoying artifacts that occur due to the discrete nature of radiological data should be corrected during this process.
- *To visualize the reconstructed vascular model* by emphasizing the topological and geometrical information as well as depth relations.
- *To provide interaction techniques to explore these visualizations*. Global filter operations and local operations should be provided to adapt the level of detail as desired.

Reconstruction and visualization are based on the model assumption that the cross section of non-pathologic vessels has a circular shape, as discussed in [MAS96]. The visualization techniques introduced here were originally developed to explore vascular structures from corrosion casts of human cadavers. Highly accurate vascular trees could be extracted from CT data of these corrosion casts, with a level of detail which is presently unobtainable for radiological data acquired from living patients. Dedicated visualization techniques were needed to explore these vascular structures. These visualizations also proved useful for therapy planning procedures. Within these procedures vascular structures are not pathologic themselves but represent important anatomic context of pathologic structures.

2 PRIOR AND RELATED WORK

Conventional methods for visualizing anatomic structures from volume data do not reconstruct vascular structures. Isosurface rendering produces artifacts: either vessels appear disconnected in the periphery or structures which do not belong to the vessels but exhibit similar intensity values are included in the visualization. For the visualization of vascular structures, Maximum Intensity Projections (MIP) are frequently used. However, MIP projections do not correctly reflect depth relations: some voxels might be displayed even though other voxels with high opacity lie nearer to the camera. Moreover, small vessels tend to disappear completely. Closest vessel projections (CVP) were introduced as a modification of MIP [ZUI95]. The CVP-projection scheme works as follows: for each ray, the first sampling point with an intensity above a user-defined threshold is projected to the image. Thus, small vessels in front of large vessels (with higher intensities) are visible. With the methods described thus far, interactive exploration of vascular structures is limited. For example, it is not possible to selectively hide or emphasize vessels.

Reconstruction of Vessels for Visualization. The benefits of reconstructing vascular structures for a visualization that emphasizes connectivity and shape features was recognized early [GER93, ERI94]. Vessels have been displayed as tubes after skeletonization [MAS96]. The skeletonization itself is done via a sophisticated algorithm based on mathematical morphology which preserves the topology and controls small side-branches of the skeleton. Smooth transitions of the tubes at branchings are not considered, however. [PUI97] introduced methods for visualizing cerebral blood vessels, focusing on shading techniques which emphasize vessel curvature and the efficient computation of such surface-based visualizations. HÖHNE *et al*. built a geometric model for anatomy education based on the Visible Human dataset [HÖH00]. Small vessels and nerves which could be detected only in part (or not at all) have been modeled by placing ball-shaped markers which are connected with B-splines to produce smooth visualizations. A semitransparent visualization of the segmented vessels overlaid with an opaque visualization of the skeleton inside the vessels was suggested in [HER00]. This method is based on a sophisticated vessel segmentation and aims at quantification of blood vessels for detecting stenosis.

Reconstruction of Vessels for Interaction. Only a few papers deal with the exploration of vascular structures. In [NIE99], vessels are segmented and analyzed in order to selectively hide them. The subdivision of vessels by placing and moving spheres in preparation for interaction with selected parts of vascular structures is described in [BAR99]. [MAR00] deals with the geometrical and morphological analysis of retinal blood images. Although it does not directly address interaction facilities, this paper describes the determination of measurements useful for interaction.

Prior Work. The work presented here builds on earlier work in our group [ZAH95]. Based on the skeletonization of vascular structures, abstract visualizations have been generated which highlight the vessel topology but ignore vessel diameters (Figure 2). Frequently, a visualization is desired which is less abstract than the left image in Figure 2. Ideally, the level of abstraction could be modified interactively.

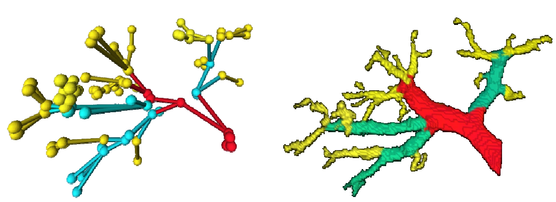

Figure 2: Abstract vessel visualization consisting of tubes and spheres (left) and „realistic“ surface-based vessel visualization (right). Colors represent the hierarchy of the vessels. (From [ZAH95]).

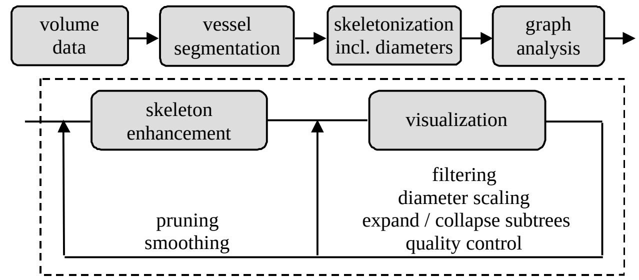

Figure 3: Vessel analysis, visualization and interaction tasks.

3 IMAGE ANALYSIS

In order to understand a vascular structure it is crucial to represent its hierarchy and make it available for interaction. Moreover, the vessel diameter is important for therapy planning: surgeons try to avoid damaging vascular structures above a certain diameter. To support the desired interaction, we use the pipeline of analysis steps illustrated in Figure 3. The first steps of the pipeline – outside the dotted box – are described in a formal manner in [SEL00]. We briefly repeat the main steps in Sect. 3.1. The interactions tasks are discussed in Sect. 5.

3.1 Vessel Analysis

Vessel Segmentation. Vessels are segmented using a fast region-growing algorithm adapted to the characteristics of thin, branching vessels. Starting from user-defined seedpoints, the algorithm accumulates all high-intensity voxels (those above a threshold). With some preprocessing (including background compensation) and a threshold suggested by the system, this algorithm works well for a large variety of radiological data.

Skeletonization. Vessels are skeletonized with a topology-preserving thinning algorithm which yields an exact centerline representation and the radius at each voxel of the skeleton.

Graph Analysis. The skeleton is transformed in a directed acyclic graph *G=(V, E)* with vertices *V* representing branchings (e.g., bifurcations or trifurcations) and edges *E* representing connections between them. For each edge, a list is kept recording the skeleton voxels and vessel diameters along it.

Identification of Different Vessel Systems. In some organs of the human body several vascular systems are present. Usually, the vessel segmentation yields voxels of all these systems. This is due to the limited resolution of the acquired data: a voxel of one vascular structure might be adjacent to a voxel belonging to another structure, and so the region-growing algorithm intrudes on the other structure. While we do not modify the vessel segmentation algorithm, we separate vessels in the graph analysis step. The basic assumption for this separation is that the vessel diameter is reduced from the root of the tree to the periphery. Points of the skeleton where this assumption is not valid are candidates for the separation of vascular structures. This process is controlled by a sensitivity parameter in order to prevent too many vascular trees from arising.

After separation, there is one graph per vessel system. The root of each graph represents the root of the corresponding vascular tree. With this data structure top-down and bottom-up traversal of vascular structures is possible.

The vessel analysis pipeline is illustrated in Figure 4.

3.2 Enhancement Of Skeletons

Due to the discrete nature of radiological data, distracting aliasing effects occur if the skeleton is immediately visualized. Several enhancement techniques are applied to eliminate these effects.

As a first step, a set P of small side branches is suppressed (*pruning*) by taking into account the length of a side branch relative to the branch at the next higher level of hierarchy (recall [MAS96]). The set P of irrelevant branches is defined as follows (B: set of all branches, b^*: parent branch of branch b, L_b: length of branch b, D_b: diameter of branch b, k: constant):

$$P = \{\ b \in B \ |\ L_b < k \cdot D_{b^*}\ \}.$$

A value of $k = 0.7$ has turned out to produce satisfactory results.

Next, a one-dimensional binomial filter with [121]-kernel is used to smooth the edges of the skeleton (see Figure 5). For all voxels of the skeleton with two neighbors (e.g. along the edges between branchings), the resulting skeleton is strongly improved. This simple smoothing causes undesirable effects at branchings, however. In the case of a small bifurcation, the main branch is pulled towards the small sidebranch, if all neighbors are weighted the same (Figure 6, top left). It seems advisable to decide which neighbors belong to the main vessel that only should be taken into account (Figure 6, top right).

Conversely, if a symmetric bifurcation occurs (at the end of a major vessel where two smaller vessels coincide), it is desirable for both smaller vessels to bifurcate with the same angle. The definition of a main vessel would not be adequate in this case (Figure 6, bottom).

Therefore, the smoothing process is modified at branchings so as to weight the voxels involved in proportion to their relevance. The size of each subtree is used to measure the relevance of the corresponding neighboring voxel. More precisely, the relevance of each neighboring voxel is identified with the total length of all subbranches depending on the respective voxel. Thus, voxels belonging to terminal branches in the vascular tree are considered least relevant.

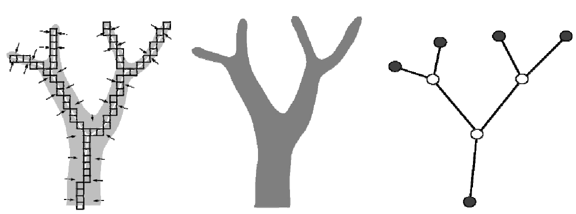

Figure 4: Vessel segmentation, skeletonization (construction of a one voxel-width representation in the centerline of the branches) and reconstruction of the branching graph illustrated in 2d.

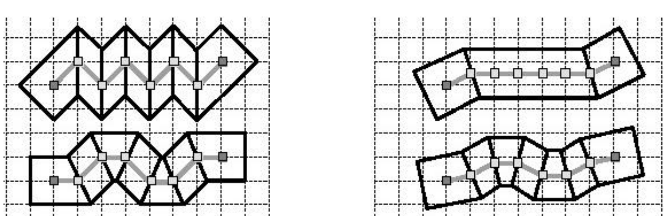

Figure 5: Smoothing with a binomial filter. The jaggy skeleton on the left is transformed into the smoother skeleton on the right. Small quadrilaterals represent the voxel centers. Note that start and endpoints of the skeleton are unaffected.

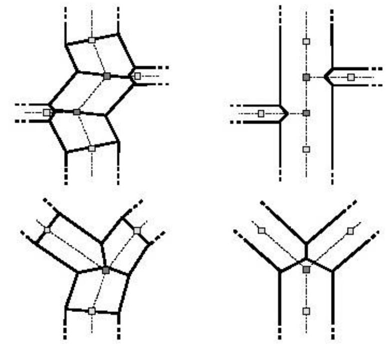

Figure 6: Undesired effects on branching structures (left) are corrected by considering the relevance of voxels (right).

4 VESSEL VISUALIZATION

An extension of OPENGL, GLEXTRUSIONS, is used to visualize vascular structures. With this library, graphics primitives of various shapes may be extruded along a path. For visualizing vascular structures, a vascular tree is mapped to a set of lists $\{L_i\}$ which comprise its sequential edges. The edges of each list represent the path used for the extrusion. Because interpolation of surface normals is applied to the edges of *one* path, it is desirable to assign as many edges as possible to a single list. If two possible paths have the same number of edges, the path with greater total length is chosen. The mapping of a vascular tree to the lists $\{L_i\}$ starts at the root and follows the longest path to a leaf node. All edges thus traced are assigned L_1. This strategy is applied recursively to each subtree until each edge belongs to a list. Figure 7 illustrates the process for a simple 2d tree.

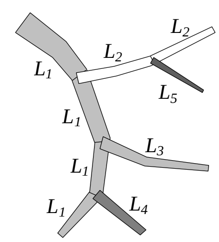

Figure 7: Sequential edges of the vascular tree are mapped to different lists as the first step for visualization via extrusions. Edges with the same gray value belong to the same list.

Concatenated graphics primitives are fitted to the path for each list. It turns out that truncated cones are able to represent local variations of the vessel diameter appropriately. We refer to this method as High Quality Vessel Visualization (HQVV).

Quality. The accuracy of the visualization of the symbolic model – which we refer to as *quality* – depends on two factors:

- the accuracy of the polygonal approximation of cones (the number of vertices per truncated cone)
- the sampling rate along the path (the number of cones generated).

Representing the circular cross section of a cone with a triangle yields minimal accuracy in the first parameter. A 20-gon representation of the circular cross section achieves maximum accuracy with GLEXTRUSIONS. Except for extremely zoomed visualizations there is no noticeable visual effect when more than 20 vertices are used. Octagons represent a reasonable tradeoff. An application programmer does not deal directly with actual polygons but uses a quality parameter in the range of 0 (mapped to a triangle) to 1 (mapped to a polygon with 20 vertices).

At the minimum sampling rate in the second parameter, one cone is generated to represent the complete path between two branchings. At the maximum sampling rate, one cone is generated between every two voxels along the path (Figure 8). Because the resulting polygon meshes remain small even for high quality values, there is usually no trade-off required between quality and speed.

Visualization of Leaf Branches. One problem with the straightforward application of cones for vessel visualization is the appearance at endpoints. Without special care vessels seem to end abruptly, rather than having a more natural smooth appearance. At the end of each path, a half-sphere is therefore included, which has the same diameter as the final cone used in the extrusions (Figure 9). Actually, the half-sphere is approximated by four truncated cones with appropriate narrowing of the diameter.

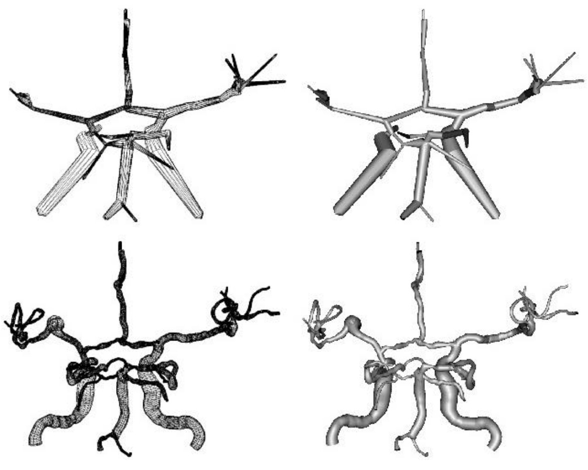

Figure 8: The vessels in the neck area are reconstructed from MR-data and visualized with different resolutions along the skeleton. The wireframe visualizations (left) correspond to the Gouraud-shaded visualizations (right).

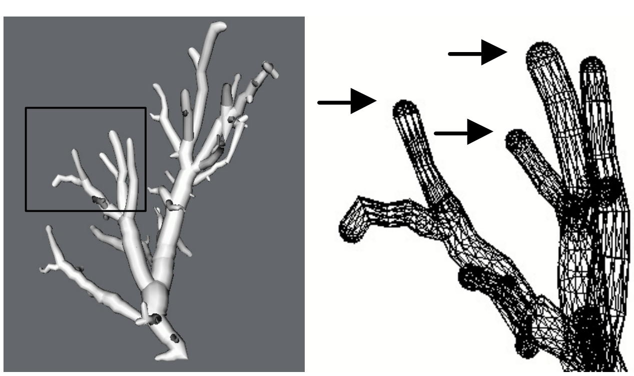

Figure 9: The right image presents a close-up view of the left image as wire-frame visualization. A (triangulated) half-sphere leads to a smooth appearance at the endpoints of vessels (indicated by arrows).

5 EXPLORATION OF VASCULATURE

For exploring vascular structures, it is essential to be able to select subtrees of a vessel tree or to select a single vessel tree. Such filter operations could be based on the vessel diameter or on the hierarchy of the vascular trees. This raises the question how the hierarchy of an asymmetric tree can be assessed. In [HAH00] this question was investigated in detail. There, the growth of vascular structures, the vessel diameters in different parts of vascular structures and the volume supplied by branches were considered. A measure was required which assigned the same value to vessels having approximately the same diameter and supply volume. The branching hierarchy in the vascular tree is not a good measure in these respects. The Strahler scheme, which assigns levels to branches in a bottom-up manner, is a simple yet accurate measure for this purpose [STR57].

The Strahler scheme has been used elsewhere to describe structural properties of vascular systems: In [KAS93] and [Bea00] the "diameter-defined Strahler system" has been defined to establish a mathematical model of pig coronary arteries for the purpose of haemodynamic analysis. In [MAR00] the Strahler scheme was utilized to characterize the structure of retinal blood vessels.

The Strahler scheme proceeds as follows: each leaf node is assigned to level 1. At a branching, the level is incremented by one if two branches with the same level coincide. If branches with different levels coincide, the level remains unchanged in the rootward direction (Figure 10). These numbers are called Strahler level in the following.

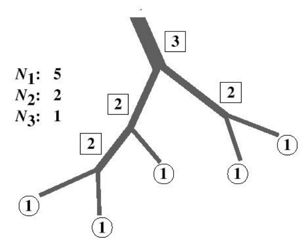

Figure 10: Definition of the Strahler scheme which is exploited to filter vessels according to the hierarchy.

5.1 Filtering

Filtering with the Strahler scheme. For filtering purposes, the Strahler levels are re-ordered: the root is assigned to level 1, and the leaf nodes are assigned to the level of the original root node (*n*). Each branch in between is assigned to level *(n+1)-m*, where *m* is the original Strahler level of the branch. A vascular tree from a corrosion cast is used to illustrate pruning based on the Strahler levels in Figure 11.

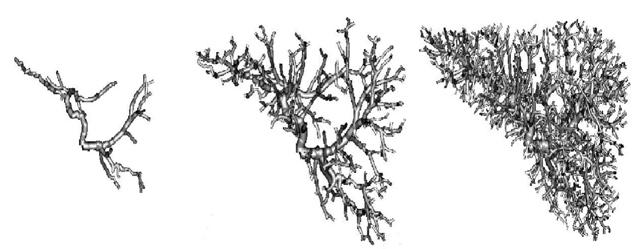

Figure 11: Pruning of a vascular tree based on the Strahler hierarchy. From left to right, vascular structures of the 3rd, 5th and 7th level are displayed.

Filtering with the Vessel Diameter. Because it meets to the mental model employed by physicians, the ability to select a subtree of vascular structures with a diameter above a threshold is very desirable. As shown in [HAH00], vessel diameter corresponds well to the Strahler levels. However, vessel diameter is very sensitive to discretization artifacts. Therefore, filter operations based on the diameter alone often result in a disconnected visualization. To ensure that vascular structures remain connected, two modifications have been investigated:

- *Bottom-up*: Starting from the leaf nodes of the tree, the first branches $\{b_i\}$ with a diameter above the threshold are searched. All branches between an element of $\{b_i\}$ and the root node are visualized even if their diameters fall below the threshold.
- *Top-down*: Starting from the root node all branches with a diameter above the threshold are visualized. When a branch b has a diameter below the threshold, the whole subtree subtending b is suppressed, even if some of its branches have a diameter above the threshold.

Note that the visualization result depends on the choice of strategy. In order to prevent suppression of branches which might be crucial, we employ the top-down strategy, which selects more branches for the same diameter.

5.2 Modification Of Presentation Variables

Filtering techniques make it possible to control the complexity of the vessel visualization. If several vascular structures are presented simultaneously, additional interaction techniques are required to get an overview. One simple yet useful technique is to select a (sub)-tree and render it semi-transparent to allow the user to look through these structures. With this technique, the visualization might focus on the remaining opaque structures (Figure 12). Alternatively, the vessel diameter and the Strahler level might also be used to assign presentation variables to the branches of a vascular tree (e. g., transparency values). In Figure 14, for example, the radius is color-coded.

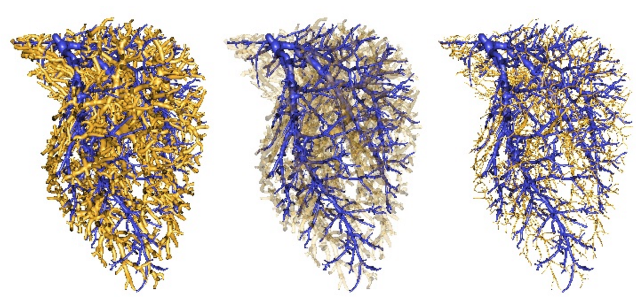

Figure 12: Different emphasis techniques are used to explore two vascular trees inside the liver (left). In the middle image, one tree (portal vein) is rendered 50% transparent. In the right image, the radius of the portal venous branches is reduced to 15%.

Diameter scaling. Another technique to control the complexity of the visualization is the scale of the vessel diameter (Figure 12, right). Linear, logarithmic, or exponential reduction of vessel diameter are common options. A linear scale is appropriate to illustrate the relations of vessel diameters.

5.3 Smoothing

The vessel diameters resulting from image analysis (recall Sect. 3) are discontinuous for typical radiological data. This results in distracting effects, which are illustrated in Figure 13. The color coding of the vessel diameter highlights this problem. It is therefore desirable to smooth the diameters; for this purpose the user can control how strongly the vessel diameter is smoothed (see Figure 14). The smoothing process is carried out with techniques similar to those used to enhance the skeleton (recall Sect. 3.2). Again, it is straightforward to apply smoothing to parts of the skeleton without branchings. Special care is taken at branchings to estimate the influence of all coincident branches.

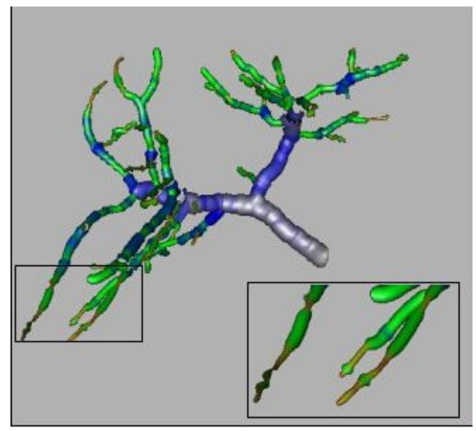

Figure 13: A vascular tree reconstructed from radiological data from a living patient. The vessel diameters are color-coded to highlight discontinuities, particularly for small vessels (see inset).

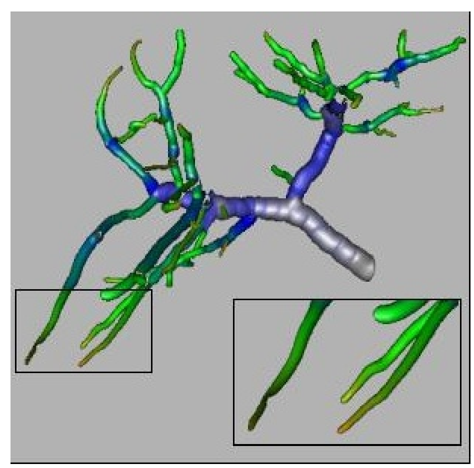

Figure 14: The same vascular tree as in Figure 13 is shown, but with smoothed diameters. The inset view reveals considerable differences for small vessels.

5.4 Expand/Collapse Subtrees

The filter operations described in Sect. 5.1 allow the user to control the visualized subset of the data globally. In order to study parts of a vascular system in more detail, local operations are required to expand or collapse subtrees.

As prerequisite for these operations, the user has to select a part of the vascular tree. However, the polygon meshes rendered cannot be interactively selected, since GLEXTRUSIONS does not support the picking mechanism of OPENGL. Therefore, the skeleton (which is located inside the polygons) is represented as a pointset and rendered as part of an OPENINVENTOR scenegraph. Although the visualization is hidden, it can be used for the selection. The point picked by the mouse pointer is „snapped“ to a voxel on the skeleton lying within a certain radius. The edge of the graph being referred can then easily be determined.

Once a branch of the vascular tree is selected, it might be expanded by one Strahler level, by two levels, or it may be completely expanded. The collapse operation always prunes the complete subtree of the selected branch.

5.5 Implementation

The visualization techniques described are integrated in an operator, SKELETONVIS, which is part of our in-house-library for image processing and visualization, ILAB ([SCH00]). All parameters described are adjustable via the user interface for this operator. ILAB contains operators for each OPENINVENTOR node. A SKELETONVIS-operator is normally connected to an OPENINVENTOR viewer for output. This provides the usual facilities for camera movement.

6 APPLICATIONS

The visualization techniques described here have been used extensively for preoperative planning in liver surgery. As one example, the improved vessel visualization is used for oncologic liver surgery, where it is essential to recognize the spatial relations around a malignant tumor and to estimate how the destruction or removal of this tumor and a safety margin around it would affect the blood supply [PRE00, PRE01]. In particular, it is crucial to know in advance which parts of a vascular system depend on a section which must be damaged.

A second example concerns living related liver transplants (LRLT), also called live donor transplantations. These operations are motivated by the shortage of organs for transplantation. In this procedure, the liver is split into two parts, one remaining in situ while the other is given to a recipient. In contrast to oncologic liver surgery, where it often suffices to remove a territory in the periphery of an organ, the liver is completely divided in an LRLT. The vascular anatomy is crucial in the evaluation of potential donors [CAL01]. As can be seen from an atlas of anatomy, there are many topologically different variations in how the hepatic arteries proceed. [NET95], for example, differentiates between eight main variants of the primary branching pattern of hepatic arteries. Also, the drainage of the liver with the hepatic vein varies considerably from patient to patient. There might be an additional so-called accessory hepatic vein which is also involved in the drainage of the liver. For donor selection and for decisions concerning the operation strategy, surgeons must carefully determine which of these variants in the vessel architecture occur, or if there is perhaps even a completely different topology. The way the liver might be divided determines the volume of liver tissue which remains and the volume of the graft. Whether or not LRLT is feasible depends largely on these volumes.

The next four images relate to applications in liver surgery planning. As a first example, the vascular anatomy of the liver is shown in Figure 15. Two colors are employed to highlight the two vascular trees. Figure 16 depicts an anatomic abnormality of a patient's portal venous system. Figure 17 illustrates the planned splitting strategy. Where the portal venous tree is divided can now be clearly seen. As the final example, three malignant tumors inside the liver are visible in Figure 18. In order to evaluate the localization of these tumors, they are integrated in a semitransparent visualization of the liver and a visualization of the portal venous tree.

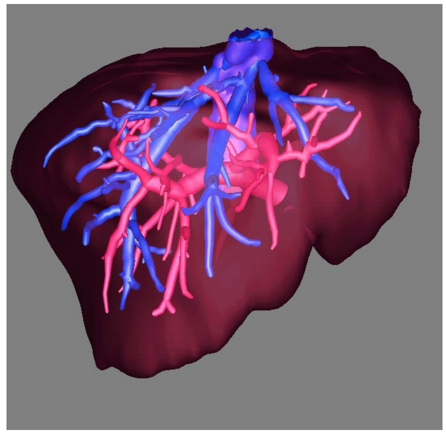

Figure 15: HQVV (High Quality Vessel Visualization) of the intrahepatic vascular anatomy (hepatic vein and portal vein). The diameter is smoothed, but not scaled.

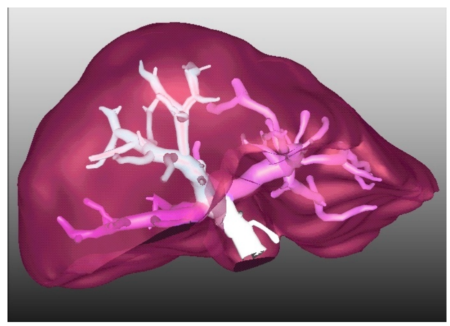

Figure 16: A patient was evaluated as potential donor for a living transplant. The HQVV-method reveals a trifurcation, a rare anatomic variant. Because of this variant an operation was considered to be too risky.

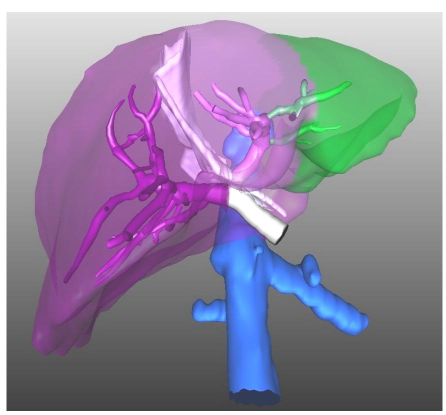

Figure 17: Planning of living-related liver transplants. The plane in the central part reflects the intended splitting position. The large aorta is visualized with (traditional) surface-based rendering. The vessels inside the liver are visualized with the HQVV-method. This visualization makes it obvious which parts of the portal venous vascular tree are affected.

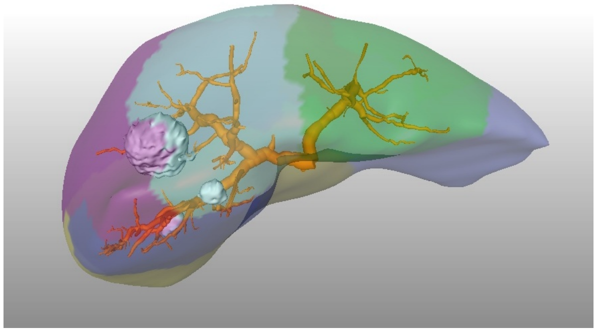

Figure 18: Visualization for tumor resection planning. Three tumors are inside the liver, which is rendered semitransparent. Vessels are visualized with the HQVV-method.

7 CONCLUSION AND FUTURE WORK

Methods for visualizing vascular structures via graphic primitives and interaction techniques for the exploration of vascular structures have been described. This paper makes two main contributions. First, skeleton and vessel diameter smoothing techniques are used to produce high-quality vessel visualizations based on concatenated truncated cones. Filtering techniques based on the Strahler scheme and interaction techniques to emphasize subtrees comprise the second major aspect. Even complex vascular trees can be clearly visualized with these interaction techniques. For clinical applications it is crucial to have interaction facilities which allow the user to focus her attention on a specific vessel system or part thereof.

The visualizations generated present a very acceptable trade-off between the goal of accurate visualization and the desire to interpret the depicted spatial relations. User control over the most relevant quality parameters is essential for producing acceptable visualizations. The image processing steps necessary to reconstruct vessels have been largely automated and are used in the clinical routine [CAL01]. The visualization techniques presented in this paper were inspired by the clear and easy-to-interpret visualizations in traditional teaching materials, in particular those intended for surgeons (recall [MAZ97]). We have attempted to create visualizations of similar quality but having two major advantages: the visualizations reveal patient-specific branching patterns, and they are intended for interaction.

Therapy planning benefits from high quality and flexible visualizations of vasculature, but their role must not be overestimated. Over and above appropriate visualizations, analysis tasks, such as determining of distances between certain structures and the approximation and volumetric analysis of vascular territories, are also useful for preoperative planning.

The main assumption underlying the visualizations of vascular structures is that they can be approximated by cones to represent a spherical cross-section. For representation of pathologic vessels, it might be superior to consider ellipsoidal cross-sections. Hybrid visualizations combining “realistic” visualizations and visualizations based on graphics primitives might be investigated as an extension of the present work. For use in the medical routine, it is desirable to automatically adapt transparency values and the scale of vessel diameters to the complexity of the data. By starting from better parameter values, interactive exploration might be more efficient with such a facility.

8 ACKNOWLEDGEMENTS

We want to thank our clinical partners, Prof. Galanski (Medical School Hannover) and Prof. Klose (University Hospital Marburg), for fruitful discussions and for excellent radiological data. Figure 8 is based on an MR-Dataset by Prof. Terwey (Institute for Magnetic Resonance Diagnosis Bremen). Figure 11 and Figure 12 are based on corrosion casts provided by Prof. Fasel (University Genf). Figure 15-17 use a dataset provided by Prof. Galanski. The images in Figure 18 use a dataset kindly provided by Prof. Klose. Many ideas for the vessel visualization were inspired by Dr. Caldarone, Dr. Frericks, Dr. Stamm and Prof. Galanski (all from Medical School Hannover). Furthermore, we want to thank Dr. Prause for fruitful discussions of these methods and for comments on the paper. W. Spindler gave valuable implementation hints and prepared some of the images used in this paper. Many thanks go to E. Sherwood for proof-reading the paper and to the anonymous reviewers for substantial hints to improve the paper.

REFERENCES

[Bar99] Dirk Bartz, Martin Skalej, Dorothea Welte, and Wolfgang Strasser. 3D-Virtual Angiography, *Computer-Assisted Radiology and Surgery*, Elsevier, pp. 44-48

[Bea00] Daniel A. Beard and James B. Bassingthwaighte. The Fractal Nature of Myocardial Blood Flow Emerges from a Whole-Organ Model of Arterial Network, *Journal of Vascular Research*, Vol. 37: 282-296

[Cal01] Franco C. Caldarone, Bernd B. Frericks, Georg Stamm et al. 3D CT Modeling of Hepatic Vessel Architecture and Volume Calculation in Living Related Liver Transplantation, Submitted to *Radiology*

[Cou57] Claude Couinaud. *Le foie – Etudes anatomiques et churgicales*, Paris, Masson

[Ehr94] Hans H. Ehricke, Klaus Donner, Walter Koller, and Wolfgang Straßer. Visualization of Vasculature from Volume Data, *Computers and Graphics*

[Ger93] Guido Gerig, Thomas Koller, Gabor Székely, Christian Brechbühler, and Olaf Kübler. Symbolic Description of 3d structures applied to cerebral vessel tree obtained from MR angiography volume data, *Proc. of Information Processing in Medical Imaging*, Springer, LNCS, Vol. 687, pp. 94-111

[Hah01] Horst Hahn, Carl J.G. Evertsz, Jean H.D. Fasel, and Heinz-Otto Peitgen. Fractal Properties, Segmental Anatomy, and Interdependence of the Human Portal Vein, *Fractals 2000 in Biology and Medicine*, Birkhäuser, Basel, in press

[Her00] Marcela Hernandez-Hoyos, Alfred Anwander, Maciej Orkisz, Jean-Pierre Roux, Philippe Douek, Isabelle Magnin. A Deformable Vessel Model with Single Point Initialization for Segmentation, Quantification and Visualization of Blood Vessels in 3d MRA, *Medical Image Computing and Computer-Assisted Intervention (MICCAI)*, Springer, LNCS, Vol. 1935, pp. 735-744

[Höh00] Karl-Heinz Höhne, Bernhard Pflesser, Andreas Pommert et al. A Realistic Model of the Inner Organs from the Visible Human Data, *Medical Image Computing and Computer-Assisted Intervention (MICCAI)*, Springer, LNCS, Vol. 1935, pp. 776-785

[Kas93] Ghassan Kassab, Carmela A. Rider, Nina J. Tang, and Yuan-Cheng B. Fung. Morphometry of pig coronary arterial trees, *American Journal of Physiology* 265: H350-H365

[Mas96] Yoshitaka Masutani, Ken Masamune, and Takeyoshi Dohi. Region-Growing-Based Feature Extraction Algorithm for Tree-Like Objects, *Visualization in Biomedical Computing* (Hamburg, September), Springer, LNCS, Vol. 1131, pp. 161-171

[Mar00] M. Elena Martinez-Perez, Alun D. Hughes, Alice V. Stanton, Simon A. Thom, Neil Chapman, Anil A. Bahrath, and Kim H. Parker. Geometrical and Morphological Analysis of Vascular Branches from Fundus Retinal Images. *Medical Image Computing and Computer-Assisted Intervention (MICCAI)*, Springer, LNCS, Vol. 1935, pp. 756-765

[Maz97] Alighieri Mazziotti, and Antonio Cavallari. *Techniques in Liver Surgery*, Greenwich Medical Media

[Net95] Frank H Netter. *Atlas of Human Anatomy*, 8th edition, Ciba Geigy Corporation, Summit New Jersey

[Nie99] Wiro J. Niessen, ADM van Swihjndregt, BHP Elsmann et al. Improved Arterial Visualization in Blood Pool Agent MRA of the Peripheral Vasculature, *Computer-Assisted Radiology and Surgery*, Elsevier, pp. 119-123

[Pre00] Bernhard Preim, Dirk Selle, Wolf Spindler, Karl J. Oldhafer, and Heinz-Otto Peitgen. Interaction Techniques and Vessel Analysis for Preoperative Planning in Liver Surgery, *Proc. of Medical Image Computing and Computer-Assisted Intervention (MICCAI)*, Springer, LNCS, Vol. 1935, pp. 608-617

[Pre01] Bernhard Preim, Wolf Spindler, Karl J. Oldhafer, and Heinz-Otto Peitgen. 3d-Interaction Techniques for Planning Oncologic Soft Tissue Operations, *Proc. of Graphics Interface* (Ottawa, June), pp. 183-190

[Pui97] Anna Puig, Dani Tost and Isabel Navazo. An Interactive Cerebral Blood Vessel Exploration System, *IEEE Visualization* (Phoenix, Arizona, October), pp. 433-436

[Sch00] Florian Schröcker, Wilhelm Berghorn, Holger Bettag, Andreas Bohne, Jens Breitenborn, Horst Hahn, Bernhard Preim et al. Highly integrated user-friendly research and development platform for medical image processing and visualization, Supplement to *Radiology* Vol. 217, November, pp. 699

[Sel00] Dirk Selle, Wolf Spindler, Bernhard Preim and Heinz-Otto Peitgen. Mathematical Methods in Medical Imaging: Analysis of Vascular Structures for Liver Surgery Planning, *Mathematic Unlimited – 2001 and Beyond*, Springer, pp. 1039-1059

[Str57] Arthur N. Strahler. Quantitative Analysis of Watershed Geomorphology, *American Geophysical Union Transactions*, Vol. 8 (6), pp. 913-920

[Zah95] Cornelia Zahlten, Hartmut Jürgens, and Heinz-Otto Peitgen. Reconstruction of Branching Blood Vessels from CT Data, *Visualization in Scientific Computing*, Springer, pp. 41-52